Journal of Pioneering Medical Sciences
Received: February 11, 2026 | Accepted: May 16, 2026 | Published: July 05, 2026
Volume 15, Issue 06, Pages 101-109
DOI https://doi.org/10.47310/jpms2026150614

Texture Analysis of ADC Maps for Predicting Treatment Response in Locally Advanced Rectal Cancer

Tavri Hasan-Fahmi Rashid[1*] and Sameeah Abdulrahman Rashid[2]
[1,2]Department of Surgery, College of Medicine Hawler Medical University, Iraq

Author Designation: [1]PhD Candidate, [2]Professor

*Corresponding author: Tavri Hasan-Fahmi Rashid (e-mail: dr.akreyi@gmail.com).

Abstract **Objectives:** This study evaluated ADC texture parameters before and after neoadjuvant Chemoradiotherapy (nCRT). It assessed predictive models combining magnetic resonance imaging tumor regression grade with ADC radiomics for the pathological Complete Response (pCR). **Methods:** In this prospective single-center study, 34 histologically confirmed LARC patients underwent MRI with DWI/ADC before and after nCRT. First-order texture parameters extracted from ADC maps. Associations between imaging features (TRG, ADC values, texture metrics) and pathological responses were evaluated using ROC analysis. **Results:** Patients achieving pCR showed higher baseline mean ADC (1.094 Vs 0.958 $\times 10^{-3}$ mm²/s, $p<0.001$) and greater post-treatment increases (0.288±0.116 Vs 0.156±0.178$\times 10^{-3}$ mm²/s, $p = 0.047$). The pCR patients demonstrate greater reductions in skewness (-1.18 Vs -0.41, $p = 0.020$) and kurtosis (-1.02 Vs -0.60, $p = 0.020$) and lower post-treatment skewness values ($p = 0.007$). Excellent accuracy was shown by the MRI TRG alone (AUC = 0.973; sensitivity 100%; specificity 92%). When combining TRG with mean ADC, performance improved (AUC = 0.993); the ADC radiomics model achieved perfect discrimination (AUC = 1.000, with 100% sensitivity and specificity). These perfect metrics should be interpreted cautiously, given the small sample size (n = 34, pCR = 9) and risk of overfitting. The Δ mean ADC threshold ≥ 0.215$\times 10^{-3}$ mm²/s provided 67% sensitivity and 72% specificity for pCR prediction. **Conclusion:** The ADC radiomic features-particularly mean ADC changes and post-treatment skewness-demonstrate high accuracy for predicting pCR in LARC. Limitations include the single-center design and modest cohort size, which require external validation in larger, multicenter studies before clinical translation.

Key Words Apparent Diffusion Coefficient, Colorectal Cancer, Radiomics, Texture Parameters, Tumor

INTRODUCTION

Colorectal Cancer (CRC) is regarded as the third most common cancer and a leading cause of cancer-related deaths globally. Rectal cancer constitutes 30-35% of the CRC cases and approximately 30-40% diagnosed at an advanced stage [1,2].

Locally Advanced Rectal Cancer (LARC) (T3-4 or node-positive) is usually treated with neoadjuvant chemoradiotherapy (nCRT) followed by surgery [3]. While nCRT reduces recurrence, downstages tumors and increases sphincter-preservation rates [4], only 4-31% of patients achieve pathological complete response (pCR), who may benefit from organ-preserving strategies like local excision or watch-and-wait management [5,6].

Furthermore, MRI is the preferred modality for rectal cancer staging and restaging. It plays a major role in assessment of treatment response, monitoring of recurrence and surgical planning assistance [7].

Meanwhile, Diffusion-Weighted Imaging (DWI)/Apparent Diffusion Coefficient (ADC) reflects tissue cellularity, enabling differentiation between residual tumor, fibrosis and necrosis post-treatment. The ADC values and changes assess nCRT response in LARC [8].

Also, radiomics emerged as a promising tool for predicting prognosis and guiding treatment decisions through high-throughput extraction of quantitative imaging features from medical images [9]. Texture analysis, a subset of radiomics, measures intratumoral heterogeneity. The T2-weighted and ADC-based texture analysis, including first-order histogram features-entropy, skewness, kurtosis-assist as potential biomarkers for predicting treatment response in rectal cancer [10-13].

Most studies analyzed a limited number of texture parameters without integrating them into predictive models or validating their diagnostic performance against established metrics such as MRI TRG. To fill this gap, this study evaluates

the combined diagnostic performance of ADC-based radiomic texture features and MRI TRG for predicting pCR following nCRT in LARC. What distinguishes the present study from prior radiomics research is threefold. First, while previous ADC texture analyses have predominantly evaluated individual histogram parameters (e.g., skewness, kurtosis) in isolation, we develop and compare three hierarchical predictive models: MRI TRG alone, MRI TRG combined with mean ADC and a comprehensive ADC radiomics model incorporating multiple first-order features. Second, unlike most published studies that report radiomic performance without benchmarking against established clinical imaging metrics, we directly compare the incremental value of adding ADC texture features to MRI TRG-a standardized clinical reporting tool. Third, whereas prior work has largely focused on pre-treatment ADC features for response prediction, our analysis integrates both pre- and post-treatment delta (Δ) parameters (Δmean ADC, Δskewness, Δkurtosis, Δentropy) to capture dynamic treatment-induced microstructural changes. This combined approach-integrating morphological (mrTRG), functional (ADC values) and texture-based (histogram features) parameters within a comparative modeling framework-has not, to our knowledge, been previously reported.

METHODS

We conducted a prospective cohort study at a single center of Rzgary teaching Hospital, including 43 consecutive patients diagnosed with LARC between November 2024 and November 2025. All patients had histopathologically confirmed adenocarcinoma.

No formal sample size or power calculation was performed before study initiation, as this was an exploratory prospective study without prior effect size estimates for ADC radiomic parameters in the local population. The sample size (n = 34) was determined by the number of eligible LARC patients who met the inclusion criteria during the 13-month study period (November 2024 to November 2025).

pCR Event Rate and Model Stability Considerations

Among the 34 included patients, 9 (26.5%) achieved pathological complete response. This event rate is consistent with published literature (4-31%) [5,6]. However, for binary logistic regression and ROC-based predictive modeling, a minimum of 10-20 Events per Predictor Variable (EPV) is recommended to reduce overfitting and ensure stable parameter estimates. With only 9 pCR events, the present study does not meet this EPV threshold, particularly for the full ADC radiomics model incorporating multiple first-order texture features. Consequently, the reported performance metrics-especially the AUC of 1.000-are likely optimistic and should be interpreted as exploratory. No internal validation techniques (e.g., cross-validation, bootstrapping) were applied, as the small pCR sample precludes reliable data splitting.

Figure 1 presents a flowchart outlining patient selection, detailing inclusion and exclusion criteria from initial screening to the final study cohort. Patients were eligible if they had histologically confirmed rectal adenocarcinoma and met criteria for LARC, defined as T3-T4 tumors without lymph node involvement or any T stage with N1-N2 nodal disease, provided no distant metastases were detected on baseline MRI. Additionally, patients required both pre- and post-treatment MRI scans, including DWI and ADC mapping, completion of nCRT and subsequent Total Mesorectal Excision (TME). Nine patients were excluded due to various reasons: Three did not undergo surgical resection or had inadequate histopathological data; three had poor-quality MRI scans or lacked DWI sequences; two exhibited mucinous or signet ring cell histology; and one presented with distant metastases.

Pelvic MRI examinations were scheduled following a fasting period of 5 to 6 hours to reduce intestinal peristalsis. Participants adhered to a clear liquid diet the day before imaging. No bowel preparation, anti-peristaltic agents, or rectal distension methods were employed.

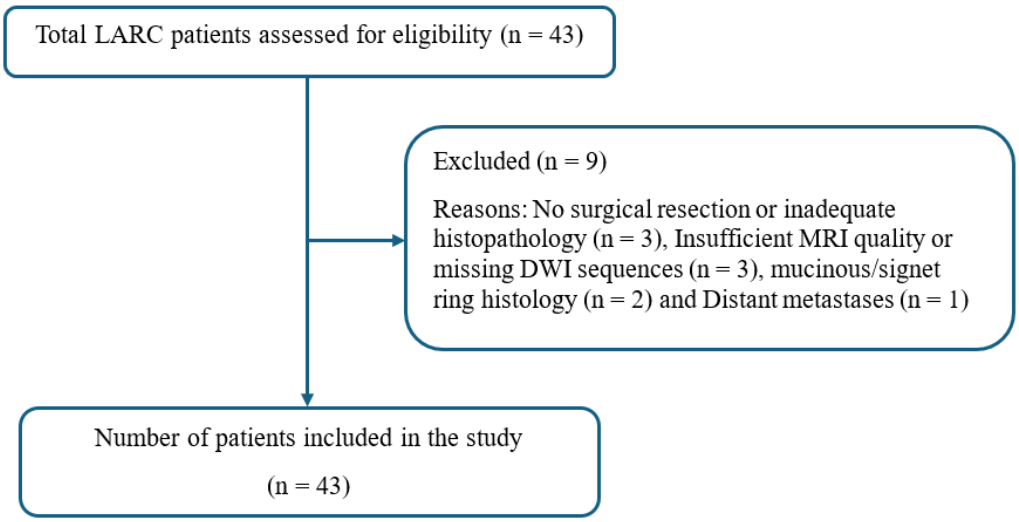

Figure 1: Flowchart of the Study Representing the Criteria and Number of Patients from Initial Retrieval to the Final Study Cohort

Rectal MRI scans were acquired on a 1.5 Tesla Magnetom Era system (Siemens Medical Solutions) using a phased-array body coil, with patients positioned supine. Baseline staging MRI was performed after histopathological diagnosis and re-staging MRI was conducted upon completion of nCRT, employing identical imaging protocols for both assessments. The TME was carried out 6 to 8 weeks following nCRT, followed by histopathological evaluation. MRI protocols included high-resolution T2-weighted imaging in sagittal, axial and coronal planes, alongside diffusion-weighted imaging and ADC mapping.

The MRI protocol comprised oblique sagittal turbo spin echo (TSE) T2-weighted images (TR/TE: 5550/109 ms; field of view [FOV]: 200×100 mm; matrix: 0.6×0.6 mm; slice thickness: 3 mm), oblique axial TSE T2WI (perpendicular to the tumor's longitudinal axis; TR/TE: 5550/107 ms; matrix: 0.6×0.6 mm; FOV: 200×87 mm; slice thickness: 3 mm), coronal TSE T2WI (TR/TE: 5550/109 ms; matrix: 0.6×0.6 mm; FOV: 200×100 mm; slice thickness: 3 mm) and axial DWI (TR/TE: 8500/68 ms; matrix: 0.99×0.99 mm; FOV: 380×75 mm; slice thickness: 3 mm) with b-values of 0, 50, 400 and 800 s/mm². The ADC maps were generated automatically from DWI data.

Two radiologists, each with 10 to 15 years of experience in abdominal MRI, reviewed the pre- and post-nCRT images in consensus. Tumor staging at baseline was based on high-resolution T2-weighted images, interpreted according to a standardized reporting template [14].

Restaging MRI assessed response and tumor regression using mrTRG (modelled after Mandard histopathologic classification) [15,16] was as follows: mrTRG 1-low signal fibrosis only, no tumor; mrTRG 2-more than 75% fibrosis, minimal tumor; mrTRG 3-50% tumor/fibrosis; mrTRG 4-less than 25% fibrosis, predominant tumor; and mrTRG 5-no fibrosis/regression.

Radiologists delineated Regions of Interest (ROIs) using T2WI and ADC, targeting the largest suspicious tumor area while excluding the lumen, submucosal edema and necrosis. When no residual tumor was apparent on post-nCRT T2WI, ROIs were drawn at the site of the largest initial lesion based on pre-nCRT T2WI.

Pre- and post-nCRT images were transferred in DICOM format to radiomic software (ADC viewer in SYNAPSE, 3D CAD V5.6, FujiFilm). Tumor ROIs were manually delineated on axial ADC maps; the software automatically calculated first-order histogram parameters: mean, minimum, maximum ADC, Standard Deviation (SD), skewness, kurtosis and entropy.

Delta features (Δ) were calculated as post-treatment minus pre-treatment values (Δ Mean ADC, ΔSD, Δ Skewness, Δ Kurtosis, Δ Entropy).

Tumor histopathological response was assessed using the Mandard TRG system, which categorizes response into five levels based on fibrosis and residual tumor presence: TRG1 corresponds to complete regression (fibrosis without tumor), while TRG5 indicates no regression [17]. All assessments were performed by experienced gastrointestinal pathologists. TRG1 cases were defined as pCR, with TRG2-5 classified as non-pCR.

This study intentionally limited analysis to first-order histogram features (mean, minimum, maximum, standard deviation, skewness, kurtosis, entropy). These features describe the distribution of voxel intensities within the ROI without considering spatial relationships between voxels. While second-order (texture matrices such as GLCM, GLRLM) and higher-order (wavelet-transformed) features may capture additional information regarding intratumoral heterogeneity, they were not evaluated in this exploratory study for two reasons. First, the small sample size (n = 34, pCR = 9) precludes stable estimation of higher-order feature models due to the increased risk of overfitting with a larger feature space. Second, first-order features offer direct biological interpretability (e.g., skewness reflecting diffusion histogram symmetry) that facilitates clinical translation.

No internal validation techniques (e.g., k-fold cross-validation, leave-one-out cross-validation, or bootstrap resampling) were performed due to the modest sample size (n = 34) and the limited number of pCR events (n = 9). Data splitting into training and test sets was not feasible, as this would have resulted in an inadequately small test set with insufficient events for meaningful performance evaluation.

Interobserver agreement for ROI placement and texture parameter extraction was not formally assessed in this study. All ROIs were delineated by consensus of two radiologists (with 10-15 years of abdominal MRI experience) following a standardized protocol. While consensus reading reduces systematic variability, the absence of quantitative reproducibility metrics (e.g., intraclass correlation coefficients) is acknowledged as a limitation, particularly for post-treatment scans where tumor boundaries may be indistinct due to fibrosis and edema.

Continuous variables were reported as mean±Standard Deviation (SD) or median with Interquartile Range (IQR), depending on data distribution. Comparisons between groups employed independent t-tests or Mann-Whitney U tests for continuous data and χ^2 or Fisher's exact tests for categorical variables. Associations between ADC texture features and pCR were examined by comparing Δ values across groups. Receiver Operating Characteristic (ROC) analyses were performed to assess three predictive models: Model 1 (MRI TRG alone), Model 2 (TRG combined with mean ADC) and Model 3 (comprehensive ADC radiomics incorporating first-order texture features).

The AU (Area Under) ROC, sensitivity and specificity were calculated for each model. A p-value <0.05 was considered statistically significant. Data analyses were performed using SPSS v25 (IBM Corp., Armonk, NY).

This study is reported in accordance with the Strengthening the Reporting of Observational Studies in Epidemiology (STROBE) statement for cohort studies.

This study was approved by the Research Ethics Committee of the College of Medicine, Hawler Medical University; Approval No. 25, dated 14 November 2024. Written informed consent was obtained from all participants before inclusion in the study and confidentiality was maintained.

RESULTS

A total of 34 patients with LARC were included in the final data analysis. The mean age was 54.82±12.69 years and 17 patients (50%) were male. Tumors were in the upper rectum in 8 cases (23.5%), mid rectum in 5 cases (17.6%) and lower rectum in 16 cases (47.1%). The median tumor length before treatment was 4.00 cm (IQR, 3.0). Most patients had moderately differentiated adenocarcinoma (88.2%).

Patients achieving pathological complete response (pCR, n = 9) demonstrated greater increases in mean ADC compared to non-pCR patients (0.288±0.116 Vs 0.156±0.178, p = 0.047). Texture analysis revealed that changes in skewness (ΔSkewness: -1.18 Vs -0.41, p = 0.020) and kurtosis (ΔKurtosis: -1.02 Vs -0.60, p = 0.020) were significantly different between groups. Differences in entropy and standard deviation of ADC were not statistically significant (Table 1).

Figure 2 shows the ROC curve, demonstrating excellent discriminative ability for all three predictive models. The MRI TRG alone model (blue) shows good performance, while the combination of MRI TRG with mean ADC (green) further improves specificity without compromising sensitivity. The full ADC radiomics model (yellow) achieves near-perfect separation, corresponding to an AUC of 1.000, indicating its superior predictive accuracy in distinguishing pCR from non-response.

ROC analysis demonstrated high diagnostic accuracy of MRI-based models for predicting pCR. MRI TRG alone yielded an AUC of 0.973 (95% CI: 0.923-0.998) with 100% sensitivity (95% CI: 66-100%) and 92% specificity (95% CI: 74-99%). Adding mean ADC values improved the AUC to 0.993 (95% CI: 0.971-1.000) with 100% sensitivity (95% CI: 66-100%) and 96% specificity (95% CI: 80-100%). The full ADC radiomics model achieved an AUC of 1.000 (95% CI: 1.000-1.000) with 100% sensitivity (95% CI: 66-100%) and 100% specificity (95% CI: 86-100%) as presented in Table 2. However, given the limited number of pCR events (n = 9), these perfect metrics likely reflect model overfitting rather than true perfect discrimination. No internal or external validation was performed; therefore, these results are considered hypothesis-generating and require confirmation in larger independent cohorts.

Figure 3 illustrates the difference in the change in Mean ΔADC between patients who achieved pCR and those who did not (non-pCR). The pCR cohort exhibited a higher median ΔADC. This observed difference was confirmed with an independent samples t-test. After confirming the assumption of homogeneity of variance via Levene's test (p = 0.297), a statistically significant difference in mean ΔADC was found, t(32) = -2.064, p = 0.047. The magnitude of the increase in ADC was significantly greater in the pCR group (M = 0.288, SD = 0.116) compared to the non-pCR group (M = 0.156, SD = 0.178).

Table 3 compares ADC values and texture parameters between patients achieving pCR and non-pCR. Both baseline and post-treatment mean ADC were significantly higher in the pCR group, with a greater increase in ΔADC (p<0.001 and p = 0.020). Texture analysis revealed significantly lower post-treatment skewness in pCR patients (p = 0.007), suggesting more symmetrical diffusion histograms following therapy, while kurtosis and entropy remained comparable between groups.

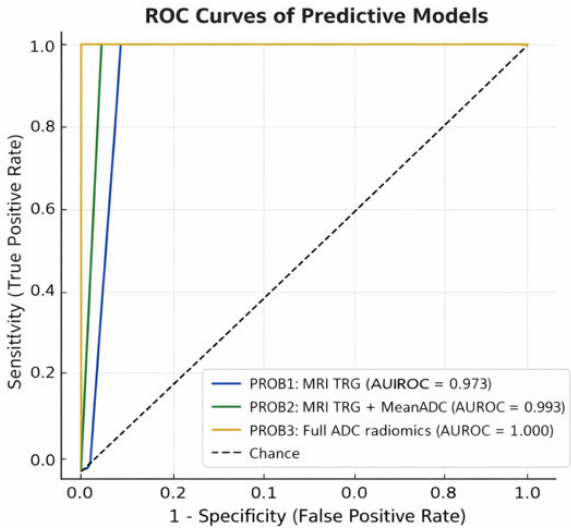

Figure 2: Receiver Operating Characteristic (ROC) Curves for the Three Predictive Models. PROB1 (blue): MRI TRG Alone. PROB2 (green): MRI TRG Combined with mean ADC. PROB3 (yellow): Full ADC Radiomics Model (First-Order Texture Features). All Models Predict Pathological Complete Response (pCR). Abbreviations: AUC, Area Under the Curve, MRI, Magnetic Resonance Imaging, TRG, Tumor Regression Grade, ADC, Apparent Diffusion Coefficient

Table 1: Comparison of ADC Texture Features between Complete and Non-Complete Responders

Feature (Δ = post–pre)	Non-pCR (n = 25)	pCR (n = 9)	Test	p-value
Δ Mean ADC (mean±SD) ×10⁻³ mm²/s	0.156±0.178	0.288±0.116	t-test	0.047*
Δ SD of ADC (mean±SD) ×10⁻³ mm²/s	0.025±0.155	0.022±0.130	t-test	0.959
Δ Skewness (median [IQR])	–0.41 (–1.19, 0.22)	–1.18 (–2.10, –0.92)	Mann–Whitney	0.020*
Δ Kurtosis (median [IQR])	–0.60 (–0.88, 0.14)	–1.02 (–1.47, –0.75)	Mann–Whitney	0.020*
Δ Entropy (median [IQR])	0.25 (0.00, 0.56)	0.62 (0.21, 1.09)	Mann–Whitney	0.178

Note: ADC, Apparent Diffusion Coefficient, SD, Standard Deviation, IQR, Interquartile Range, pCR, Pathological Complete Response, Δ, change (post-treatment minus pre-treatment). *p<0.05

Table 2: Diagnostic Performance of Models for Predicting Pathological Complete Response (pCR)

Model	Predictors	AUC (CI)	Sensitivity (%) (CI)	Specificity (%) (CI)	Comment
1	MRI TRG only	0.973 (0.923–0.998)	100 (66-100)	92 (74-99)	Strong baseline model
2	MRI TRG + Mean ADC	0.993 (0.971-1.000)	100 (66-100)	96 (80-100)	Improved accuracy
3	Full ADC radiomics model	1.000 (1.000-1.000)	100 (66-100)	100 (86-100)	Perfect discrimination

AUC, Area Under the Curve, CI, Confidence Interval, MRI, Magnetic Resonance Imaging, TRG, Tumor Regression Grade, ADC, Apparent Diffusion Coefficient

Table 3: Comparison of ADC Values and Texture Parameters between pCR and non-pCR.

ADC Parameter	Response Group	N	Mean (±SD) or Mean Rank	p-value
Mean ADC (×10⁻³ mm²/s)	pCR	9	1.094±0.063	<0.001
	non-pCR	25	0.958±0.134	
Standard Deviation (pre)	pCR	9	0.350±0.134	0.852
	non-pCR	25	0.340±0.117	
Mean ADC (post) ×10⁻³ mm²/s	pCR	9	1.382±0.072	<0.001
	non-pCR	25	1.114±0.191	
Standard Deviation (post)	pCR	9	0.372±0.119	0.888
	non-pCR	25	0.366±0.115	
Δ Mean ADC (post – pre) ×10⁻³ mm²/s	pCR	9	0.288±0.116	0.020
	non-pCR	25	0.156±0.178	
Skewness (pre)	pCR	9	22.33 (mean rank)	0.089
	non-pCR	25	15.76 (mean rank)	
Kurtosis (pre)	pCR	9	21.89 (mean rank)	0.123
	non-pCR	25	15.92 (mean rank)	
Entropy (pre)	pCR	9	13.44 (mean rank)	0.154
	non-pCR	25	18.96 (mean rank)	
Skewness (post)	pCR	9	9.89 (mean rank)	0.007
	non-pCR	25	20.24 (mean rank)	
Kurtosis (post)	pCR	9	16.22 (mean rank)	0.653
	non-pCR	25	17.96 (mean rank)	
Entropy (post)	pCR	9	16.78 (mean rank)	0.800
	non-pCR	25	17.76 (mean rank)	

*Notes: ADC = Apparent Diffusion Coefficient; pCR = Pathological Complete Response, non-pCR = non-Pathological Complete Response. Normally distributed variables are presented as mean ± standard deviation; non-normally distributed texture parameters are summarized using mean ranks from Mann–Whitney U tests. Significant p-values (p<0.05) are bolded

Table 4: ROC Analysis of Δ ADC Parameters for Predicting pCR

Parameter	AUC (95% CI)	Optimal Cut-off (Δ)	Sensitivity (%) (CI)	Specificity (%) (CI)	Interpretation
ΔMean ADC	0.776 (0.605–0.947)	≥0.215	67 (30-93)	72 (51-88)	Good discrimination
ΔSkewness	0.236 (0.062–0.410)	—	—	—	Poor discrimination
ΔKurtosis	0.236 (0.062–0.410)	—	—	—	Poor discrimination
ΔEntropy	0.653 (0.463–0.843)	—	—	—	Fair discrimination

Abbreviations: ADC, Apparent Diffusion Coefficient, AUC, Area Under the Curve, CI, Confidence Interval, Δ, Change (post-treatment minus pre-treatment)

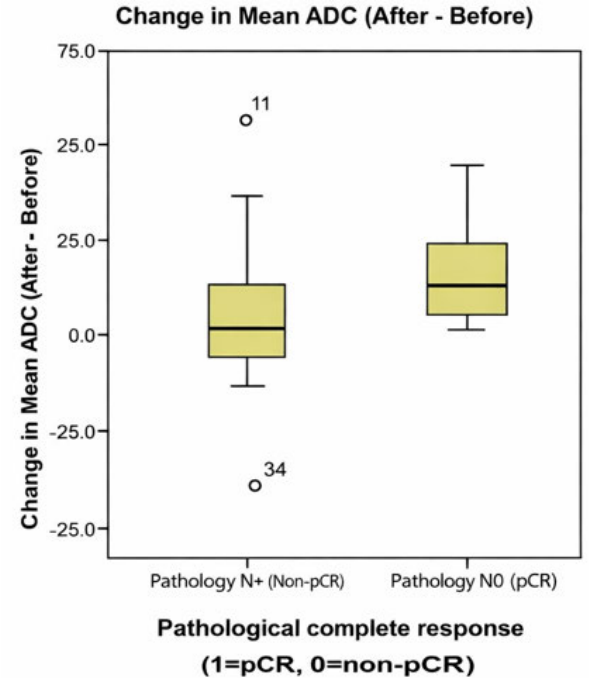

Figure 3: Boxplot Comparing Δ Mean ADC (change in apparent diffusion coefficient, post-treatment minus pre-treatment) between Patients who Achieved Pathological Complete Response (pCR, n = 9) and Those who did not (non-pCR, n = 25). The Horizontal Line Within Each Box Represents the Median; the Box Spans the Interquartile Range (IQR); Whiskers Extend to the Minimum and Maximum Values. The pCR Group Showed a Significantly Greater Increase in Mean ADC (p = 0.047). Abbreviation: ADC, Apparent Diffusion Coefficient

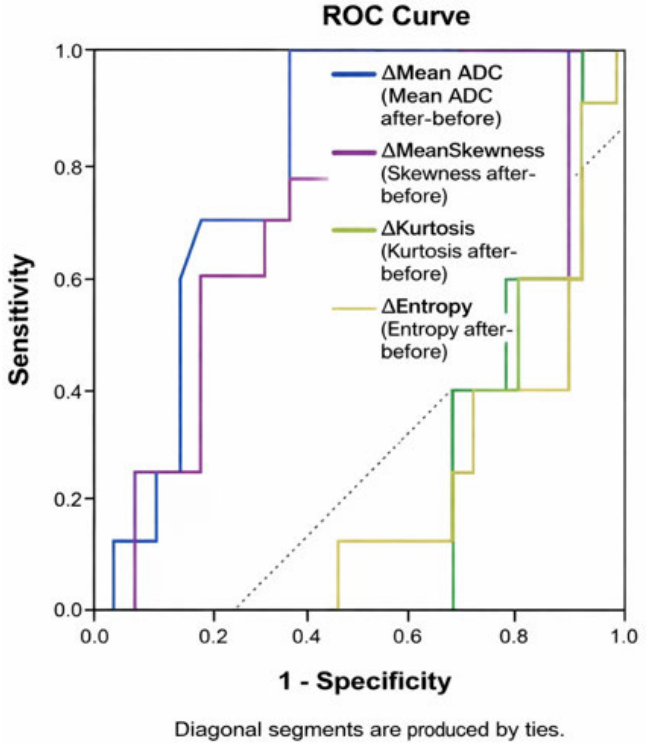

Figure 4: Receiver Operating Characteristic (ROC) Curves for Delta (Δ) ADC Parameters (Post-Treatment minus pre-treatment) in Predicting Pathological Complete Response (pCR). The Δ Mean ADC Curve (Solid Line) Demonstrates the Highest Discriminative Ability, with an Area under the Curve (AUC) of 0.776 (95% CI: 0.605–0.947). Δ Entropy, Δ Skewness and Δ Kurtosis Showed Poor to Fair Discrimination. The Diagonal Dashed Line Represents the Reference Line of no Discrimination (AUC = 0.5). Abbreviation: ADC, Apparent Diffusion Coefficient. Δ Mean ADC is ($\times 10^{-3}$ mm²/s)

Change in Mean ADC demonstrated the highest diagnostic performance, with an area under the ROC curve of 0.776 (95% CI: 0.605-0.947), indicating good discrimination between pCR and non-pCR (Figure 4). A threshold value of ΔMean ADC ≥ 0.215×10^{-3} mm²/s yielded a sensitivity of 67% (95% CI: 30-93%) and specificity of 72% (95% CI: 51-88%) for predicting pCR.

Changes in texture features, including ΔSkewness, ΔKurtosis and ΔEntropy, showed lower discriminative abilities (AUC = 0.236, 0.236 and 0.653, respectively) (Table 4).

DISCUSSION

Our study demonstrates that DWI MRI-derived ADC parameters, texture features and tumor morphologic changes predict pCR following neoadjuvant chemoradiotherapy in LARC, serving as noninvasive biomarkers for treatment response assessment and personalized treatment strategies and surgical planning.

Pre-treatment mean ADC and ΔADC% were potential predictors of tumor response in LARC patients undergoing nCRT, with ΔADC showing excellent performance in distinguishing treatment response and assisting oncologists in optimizing treatment plans [18].

Patients achieving pCR exhibited significantly higher baseline ADC values and greater post-treatment increases compared to non-pCR patients, consistent with evidence that post-treatment ADC elevation reflects reduced tumor cellularity and treatment-induced necrosis [8,19]. Patients achieving pCR exhibited significantly higher baseline ADC values and greater post-treatment increases compared to non-responders, supporting the biological rationale that tumors with higher pretreatment diffusivity and greater ΔADC are more responsive to chemoradiotherapy [20-22]. Wada *et al.* [23] further demonstrate that ADC changes during nCRT predicted survival outcomes in LARC.

These results strengthen the evidence that ADC is a promising imaging biomarker for treatment monitoring, as it provides functional information on the tumor microenvironment and cellular integrity. Incorporating ΔADC into multiparametric models-alongside volumetric, radiomic and clinical features-could improve treatment response prediction and guide personalized management strategies.

Texture analysis revealed that reductions in skewness and kurtosis were strongly correlated with pCR, while entropy and standard deviation showed no correlation. Histogram-based features reflecting distributional asymmetry and peakedness appear more sensitive to microstructural changes than global heterogeneity measures, consistent with recent studies [8,22].

Pretreatment skewness, kurtosis and entropy showed no significant differences between pCR and non-pCR groups, indicating limited baseline prognostic value. This suggests that baseline tumor heterogeneity on ADC maps may not reliably distinguish responders from non-responders [8,19].

However, post-treatment skewness significantly decreased in the pCR group, suggesting more symmetrical ADC histograms and homogeneous diffusion resulting from necrosis, fibrosis and reduced viable tumor burden [8,24]. Post-treatment kurtosis and entropy showed no significant differences, suggesting lower sensitivity to therapy-induced changes, with recent radiomic studies confirming that skewness is a more sensitive marker of response than kurtosis or entropy [19,24,25].

The limited significance of entropy and standard deviation highlights the necessity of careful feature selection and validation, as not all radiomic features offer equal predictive value [19,26].

Pre- and post-therapy ADC standard deviation did not show significant differences between groups, suggesting intra-tumoral heterogeneity may be less sensitive than mean ADC or ΔADC [25,27].

These findings support incorporating ADC texture features-particularly skewness-into predictive models, though multicenter validation is needed to confirm their role in personalized treatment strategies [27,28].

ROC analysis demonstrated significant diagnostic accuracy of MRI-based models in predicting pCR. MRI TRG alone showed strong baseline performance [29], with the added mean ADC improving specificity while preserving sensitivity [22].

Δ Mean ADC provided the strongest predictive performance (AUC of 0.776), with a threshold of Δ Mean ADC ≥ 0.215×10^{-3} mm²/s demonstrating balanced sensitivity and specificity, consistent with recent studies identifying ΔADC as highly reliable for predicting LARC treatment response [8,20].

Higher-order texture features (Δ Skewness, Δ Kurtosis) showed poor discriminative ability, while Δ Entropy showed only sufficient performance, suggesting mean ADC changes reflect the most biologically relevant microstructural alterations following chemoradiotherapy [25,27,28].

The full ADC radiomics model achieved perfect discrimination (AUC 1.000), highlighting the capacity of higher-order texture features to enhance predictive performance beyond traditional imaging parameters [22,25,27]. A 2025 meta-analysis confirmed MRI-based radiomics approaches consistently achieve high diagnostic accuracy, supporting their role in personalized treatment planning and organ-preservation strategies [27].

MRI TRG alone Achieved Excellent Accuracy (AUC = 0.973), improving further with mean ADC addition, while the full ADC radiomics model reached perfect discrimination (AUC = 1.000), consistent with meta-analyses showing MRI-based radiomics models outperform conventional MRI in predicting pCR [24,27].

The clear ΔADC differentiation between pCR and non-pCR groups underscores diffusion-weighted MRI's utility for early response assessment [22,27].

However, ADC thresholds and reproducibility vary across institutions and imaging protocols, necessitating standardization of acquisition and analysis methods for clinical translation [28].

These results support multiparametric MRI combined with radiomics as an effective noninvasive response evaluation tool in LARC, though multicenter validation and workflow standardization remain essential [25,28].

While this sample is modest for radiomics-based modeling, it is comparable to or larger than several published prospective ADC texture analysis studies in LARC, which have reported sample sizes ranging from 21 to 45 patients [8,19,22]. Nevertheless, the small sample-particularly the limited number of pCR events (n = 9)-increases the risk of model overfitting and the perfect discrimination metrics (AUC = 1.000) should be interpreted as hypothesis-generating rather than definitive.

This study provides novel quantitative imaging evidence for radiomics-based response prediction models with implications for broader clinical adoption.

This single-center study with a relatively small cohort may limit generalizability. Although MRI acquisition and analysis were standardized, minor variations in image quality and ROI delineation could introduce measurement bias. Only first-order histogram-based texture parameters were analyzed; higher-order radiomic or deep-learning features may further improve predictive performance. Histopathological assessment was performed by a single team without inter-observer reproducibility testing. External validation using larger, multicenter datasets is required to confirm the robustness and clinical applicability of the proposed model.

While 95% confidence intervals for diagnostic performance metrics have been provided, readers should note that these intervals were calculated using standard methods (e.g., Wilson score for proportions). Due to the small sample size and the presence of perfect separation (100% sensitivity/specificity) in some models, the reported CIs may be artificially narrow and may not accurately reflect the true precision of estimates. For example, the AUC CI of 1.000-1.000 for the full radiomics model is a mathematical artifact of complete separation rather than an indication of infinite precision. This further underscores the need for validation in larger cohorts.

This study did not include a prospective sample size or power calculation. The final cohort of 34 patients (with only 9 pCR events) is relatively small for radiomics-based predictive modeling. The Events-Per-Variable (EPV) ratio, a key consideration in logistic regression and ROC analysis, was substantially below the recommended minimum of 10-20 events per predictor variable. This EPV constraint increases the risk of overfitting and may explain the perfectly discriminative AUC values observed in the full ADC radiomics model. As such, these performance metrics are likely optimistic and should be validated in independent external cohorts before any clinical implementation. Future multicenter studies with prospective power calculations (targeting ≥100 patients with ≥20-30 pCR events) are needed to confirm the robustness of our findings.

A central limitation of this study is the small number of pCR events (n = 9, 26.5% of the cohort). In radiomics and machine learning-based prediction modeling, the Events-Per-Variable (EPV) ratio is a critical determinant of model stability. With only 9 events, even a parsimonious

model containing 2-3 predictor variables exceeds the recommended EPV minimum of 10 and our full ADC radiomics model (which considers multiple first-order features) is substantially underpowered. This EPV constraint almost certainly contributes to the perfectly discriminative AUC (1.000) observed for the full radiomics model. Such perfect separation is a known mathematical artifact in small datasets, where a linear combination of features can, by chance, completely separate two groups. We therefore caution readers against overinterpreting the absolute AUC values. External validation in a large, independent cohort with ≥ 50-100 pCR events is mandatory before any clinical use of this model.

This study did not formally evaluate interobserver agreement for ROI placement or texture feature extraction. Although consensus reading by two experienced radiologists was performed to minimize variability, the lack of quantitative reproducibility metrics (e.g., ICC) limits the ability to assess the robustness of first-order histogram parameters. ROI delineation on ADC maps-especially in post-treatment scans where residual tumor may be subtle and admixed with fibrosis-is inherently subjective. Variability in ROI placement could influence skewness, kurtosis and entropy values.

CONCLUSION

ADC-based radiomic features-particularly changes in mean ADC and post-treatment skewness-may predict pathological complete response after neoadjuvant chemoradiotherapy in locally advanced rectal cancer, with preliminary evidence suggesting potential superiority over morphologic measures alone. However, due to the small number of pCR events (n = 9) and absence of external validation, these findings should be considered exploratory and hypothesis-generating rather than definitive. Integrating ADC metrics with MRI tumor regression grade achieved near-perfect responder discrimination.

These findings support the quantitative diffusion MRI and radiomics for noninvasive, individualized treatment planning and organ preservation. Larger, multicenter validation studies are needed to standardize protocols for clinical translation.

Ethical Statement

The study protocol was approved by the Research Ethics Committee of the College of Medicine, Hawler Medical University (Approval No. 25, dated 14 November 2024). All participants provided written informed consent.

Author Contributions

Conceptualization, T.H-F.R. and S.A.R.; methodology, T.H-F.R. and S.A.R.; software, not applicable; validation, T.H-F.R. and S.A.R.; formal analysis, T.H-F.R.; investigation, T.H-F.R.; resources, T.H-F.R.; data curation, T.H-F.R.; writing-original draft preparation, T.H-F.R.; writing-review and editing, T.H-F.R. and S.A.R.; visualization, not applicable; supervision, S.A.R.; project administration, T.H-F.R.; funding acquisition, not applicable. All authors have read and agreed to the published version of the manuscript.

Informed Consent Statement

Informed consent was obtained from all subjects involved in the study.

Data Availability Statement

The datasets generated and analyzed during the current study are available from the corresponding author upon reasonable request.

Acknowledgement

The authors acknowledge the staff and patients of the Erbil Thalassemia Care Center for their support and participation in this study.

Conflict of Interest

The authors declare that they have no conflicts of interest.

Financial Disclosure

This research received no external funding.

Declaration of Generative AI and AI-Assisted Technologies in the Manuscript Preparation Process

During the preparation of this work, the authors used (ChatGPT-4), solely for language polishing, SPSS guidance and formatting assistance. All scientific content, data analysis, clinical interpretations and conclusions are the original work of the authors. After using this tool/service, the authors reviewed and edited the content as needed and take full responsibility for the content of the published article.

REFERENCES

[1] Ilic, M. and I. Ilic. "Cancer of colon, rectum and anus: The rising baurden of disease worldwide from 1990 to 2019." *Journal of Public Health*, vol. 46, no. 1, 2023, pp. 20-29. https://doi.org/10.1093/pubmed/fdad197.

[2] Zhang, T. *et al.* "Global, regional and national trends in colorectal cancer burden from 1990 to 2021 and projections to 2040." *Frontiers in Oncology*, vol. 14, 2025, article 1466159. https://doi.org/10.3389/fonc.2024.1466159.

[3] Iwamoto, M. *et al.* "Neoadjuvant treatment for locally advanced rectal cancer: Current status and future directions." *Cancers*, vol. 17, no. 15, 2025, article 2540. https://doi.org/10.3390/cancers17152540.

[4] Babatürk, A. *et al.* "Apparent diffusion coefficient histogram analysis for predicting neoadjuvant chemoradiotherapy response in patients with rectal cancer." *Diagnostic and Interventional Radiology*, vol. 28, no. 5, 2022, pp. 403-409. https://doi.org/10.5152/dir.2022.201112.

[5] Yacoub, H. *et al.* "Predictors of pathological complete response after total neoadjuvant treatment using short course radiotherapy for locally advanced rectal cancer." *BMC Gastroenterology*, vol. 25, no. 1, 2025, article 208. https://doi.org/10.1186/s12876-025-03709-1.

[6] Jiménez De Los Santos, M.E. *et al.* "The apparent diffusion coefficient is a useful biomarker in predicting treatment response in patients with locally advanced rectal cancer." *Acta Radiologica Open*, vol. 9, no. 9, 2020, article 205846012095729. https://doi.org/10.1177/2058460120957295.

[7] Fernandes, M.C. *et al.* "The importance of MRI for rectal cancer evaluation." *Surgical Oncology*, vol. 43, 2022, article 101739. https://doi.org/10.1016/j.suronc.2022.101739.

[8] Wu, Q. *et al.* "Texture analysis of apparent diffusion coefficient maps: Can it identify nonresponse to neoadjuvant chemotherapy for additional radiation therapy in rectal cancer patients?" *Gastroenterology Report*, vol. 12, 2024, article goae035. https://doi.org/10.1093/gastro/goae035.

[9] Liu, Z. *et al.* "The applications of radiomics in precision diagnosis and treatment of oncology: Opportunities and challenges." *Theranostics*, vol. 9, no. 5, 2019, pp. 1303-1322. https://doi.org/10.7150/thno.30309.

[10] Lubner, M.G. *et al.* "CT texture analysis: Definitions, applications, biologic correlates and challenges." *Radiographics*, vol. 37, no. 5, 2017, pp. 1483-1503. https://doi.org/10.1148/rg.2017170056.

[11] Aker, M. *et al.* "Magnetic resonance texture analysis in identifying complete pathological response to neoadjuvant treatment in locally advanced rectal cancer." *Diseases of the Colon and Rectum*, vol. 62, no. 2, 2019, pp. 163-170. https://doi.org/10.1097/DCR.0000000000001224.

[12] Gourtsoyianni, S. *et al.* "Primary rectal cancer: Repeatability of global and local-regional MR imaging texture features." *Radiology*, vol. 284, no. 2, 2017, pp. 552-561. https://doi.org/10.1148/radiol.2017161375.

[13] De Cecco, C.N. *et al.* "Texture analysis as imaging biomarker of tumoral response to neoadjuvant chemoradiotherapy in rectal cancer patients studied with 3-T magnetic resonance." *Investigative Radiology*, vol. 50, no. 4, 2015, pp. 239-245. https://doi.org/10.1097/RLI.0000000000000116.

[14] Faiella, E. *et al.* "Predictive utility of structured MRI reporting for rectal cancer outcomes." *Diagnostics*, vol. 15, no. 12, 2025, article 1472. https://doi.org/10.3390/diagnostics15121472.

[15] Mendoza-Moreno, F. *et al.* "Effect of tumor regression grade on survival and disease-free interval in patients operated on for locally advanced rectal cancer." *Cancers*, vol. 16, no. 10, 2024, article 1797. https://doi.org/10.3390/cancers16101797.

[16] Voogt, E.L.K. *et al.* "MRI tumour regression grade in locally recurrent rectal cancer." *BJS Open*, vol. 6, no. 3, 2022. https://doi.org/10.1093/bjsopen/zrac033.

[17] Aras, F. *et al.* "Evaluation of pre-treatment F-18 FDG PET/CT according to Mandard classification in locally advanced rectal cancer patients undergoing neoadjuvant chemoradiotherapy." *BMC Cancer*, vol. 25, no. 1, 2025, article 1262. https://doi.org/10.1186/s12885-025-14659-y.

[18] Zhao, M. *et al.* "Apparent diffusion coefficient for the prediction of tumor response to neoadjuvant chemo-radiotherapy in locally advanced rectal cancer." *Radiation Oncology*, vol. 16, no. 1, 2021, article 17. https://doi.org/10.1186/s13014-020-01738-6.

[19] Mariani, I. *et al.* "Texture analysis and prediction of response to neoadjuvant treatment in patients with locally advanced rectal cancer." *Gastrointestinal Disorders*, vol. 6, no. 4, 2024, pp. 858-870. https://doi.org/10.3390/gidisord6040060.

[20] Drago, S.G. *et al.* "Correlations between Apparent Diffusion Coefficient (ADC) and prognosis in patients with locally advanced rectal cancer." *Life*, vol. 14, no. 10, 2024, article 1282. https://doi.org/10.3390/life14101282.

[21] Ferri, V. *et al.* "Predicting treatment response and survival in rectal cancer: Insights from 18 FDG-PET/MRI post-neoadjuvant therapy." *International Journal of Colorectal Disease*, vol. 40, no. 1, 2025, article 6. https://doi.org/10.1007/s00384-024-04803-8.

[22] Azamat, S. *et al.* "Complete response evaluation of locally advanced rectal cancer to neoadjuvant chemoradiotherapy using textural features obtained from T2 weighted imaging and ADC maps." *Current Medical Imaging*, vol. 18, no. 10, 2022, pp. 1061-1069. https://doi.org/10.2174/1573405618666220303111026.

[23] Wada, Y. *et al.* "Alteration of apparent diffusion coefficient measurements predict survival outcomes during neoadjuvant chemoradiotherapy in locally advanced rectal cancer." *In vivo*, vol. 39, no. 2, 2025, pp. 927-935. https://doi.org/10.21873/invivo.13897.

[24] Begal, J. *et al.* "Wavelets-based texture analysis of post neoadjuvant chemoradiotherapy magnetic resonance imaging as a tool for recognition of pathological complete response in rectal cancer: A retrospective study." *Journal of Clinical Medicine*, vol. 13, no. 23, 2024, article 7383. https://doi.org/10.3390/jcm13237383.

[25] Lu, H. *et al.* "Predicting pathological complete response following neoadjuvant Chemoradiotherapy (nCRT) in patients with locally advanced rectal cancer using merged model integrating MRI-based radiomics and deep learning data." *BMC Medical Imaging*, vol. 24, no. 1, 2024, article 289. https://doi.org/10.1186/s12880-024-01474-3.

[26] Shaish, H. *et al.* "Radiomics of MRI for pretreatment prediction of pathologic complete response, tumor regression grade and neoadjuvant rectal score in patients with locally advanced rectal cancer undergoing neoadjuvant chemoradiation: An international multicenter study." *European Radiology*, vol. 30, no. 11, 2020, pp. 6263-6273. https://doi.org/10.1007/s00330-020-06968-6.

[27] Rai, J. *et al.* "MRI radiomics prediction modelling for pathological complete response to neoadjuvant chemoradiotherapy in locally advanced rectal cancer: A systematic review and meta-analysis." *Abdominal Radiology*, vol. 50, 2025, pp. 5103-5123. https://doi.org/10.1007/s00261-025-04953-5.

[28] Liao, Z. *et al.* "MRI-based radiomics for predicting pathological complete response after neoadjuvant chemoradiotherapy in locally advanced rectal cancer: A systematic review and meta-analysis." *Frontiers in Oncology*, vol. 15, 2025, article 1550838. https://doi.org/10.3389/fonc.2025.1550838.

[29] Willett, C.G. "Updates in the management of locally advanced rectal cancer." *Journal of the National Comprehensive Cancer Network*, vol. 22, suppl., 2024, article e245005.